

Determining Ionic Conductivity from Structural Models of Fast Ionic Conductors

St. Adams¹ and J. Swenson²

¹*MKI Universität Göttingen, Goldschmidtstrasse 1, 37077 Göttingen, Germany*

²*Department of Applied Physics, Chalmers University of Technology, S-412 96 Göteborg, Sweden*

(Received 20 September 1999)

Reverse Monte Carlo produced structural models of silver ion conducting glasses and crystals have been investigated by the bond-valence technique. Both absolute ionic conductivity and activation energy can be determined directly from the “pathway volume” of the structural models, i.e., from the volume fraction of the percolating pathway cluster. This pathway volume–conductivity relation was found to hold for glassy and crystalline systems with silver ion conductivities differing by more than 11 orders of magnitude. Earlier, less universal rules were rationalized and unified by means of this approach.

PACS numbers: 66.30.Hs, 61.43.Fs, 66.30.Dn

Superionic solids show the remarkable behavior of a selective ion mobility in an otherwise nearly frozen material. Apart from a few crystalline materials such as Rb_4AgI_5 , the highest ionic conductivity at room temperature (up to nearly 10^{-1} S/cm) has been observed in AgI doped glasses and composites [1,2]. The glassy conductors are of particular interest for technological applications (e.g., as solid electrolyte in electrochemical devices such as batteries, sensors, “smart windows,” etc.) due to their ease of preparation, their stability, and the large available composition ranges. In order to understand the diffusion mechanism, it is essential to find a connection between the microscopic structure and the ionic conductivity.

Several transport models, such as the weak electrolyte model [3], the random site model [4], the dynamic structure model [5], the diffusion pathway model [6–8], the cluster model [9–11], and the cluster-bypass model [12], have been proposed to explain the high ionic conductivity of superionic glasses. Most of the models involve specific or indirect assumptions about the microscopic structure in general and the distribution and local environment of the mobile cations in particular. Thus, in order to evaluate the different models and to understand the origin of the diffusion mechanism it is essential to obtain more insight about the structure and the nature of the conduction pathways. So far, our understanding of ion conduction in glasses is basically limited to some general rules and empirical relations. The conductivity is favored by a large and highly polarizable anion, e.g., I^- , in combination with a relatively small and polarizable metal ion, e.g., Ag^+ . It is also well known that a mixture of glass formers is favorable for ionic conduction [13], while mixing of mobile cations is detrimental (the mixed mobile ion effect) [14,15]. Furthermore, a strong empirical relation between conductivity enhancement and the expansion of the glass matrix, induced by the salt doping, has been observed for various oxide glasses [16].

In this Letter we show, for the first time, how the ionic conductivity can be determined directly from reasonably accurate structural models of superionic solids. We have

applied the bond-valence method [17–20] onto reverse Monte Carlo (RMC) [21] produced structural models of Ag-based superionic glasses and crystals whose conductivities differ by more than 11 orders of magnitude, and we are able to predict their dc conductivities and activation energies directly from the models. The here-proposed structure-conductivity relation is an important advancement compared to the more simple network expansion-conductivity relation presented in Ref. [16] for two main reasons. First, the present relation is not restricted to salt doped glasses; it also predicts the conductivity of undoped glasses with completely different types of networks as well as crystalline superionic phases. Second, using this relation in combination with a detailed inspection of the structural models gives us an understanding of how the microscopic structure affects the ionic conductivity.

Bond-valence sum calculations are widely used in crystallography to evaluate the plausibility of structure models (see, e.g., Ref. [20]). The bond-valence sum of an Ag^+ ion may be expressed as

$$V = \sum_X s_{\text{Ag}-X}, \quad (1)$$

where individual bond-valences $s_{\text{Ag}-X}$ for bonds to each anion are calculated by employing tabulated empirical bond-length bond-valence parameter sets, mostly of the type

$$s_{\text{Ag}-X} = \exp\left[\frac{R_0 - R}{b}\right]. \quad (2)$$

We selected a parameter set by Radaev, Fink, and Trömel [22], given by $R_0 = 1.89 \text{ \AA}$, $b = 0.33 \text{ \AA}$ for Ag-O bonds and $R_0 = 2.08 \text{ \AA}$, $b = 0.53 \text{ \AA}$ for Ag-I bonds, because, in contrast to most other literature data sets, it accounts for the influence of higher coordination shells (i.e., larger interatomic distances) and for the anion polarizability (via an appropriate choice of b). Assuming that the ion transport from one equilibrium site to the next follows pathways along which the valence mismatch $|\Delta V| = |V - V_{\text{ideal}}|$

remains as small as possible, bond-valence maps have been successfully employed to model migration pathways of mobile ions in crystalline solid electrolytes [17–19].

Bond-valence models of conduction pathways based on RMC models necessarily differ from time- and space-averaged structure models such as crystal structure data or the energy-minimized models produced by force-field calculations. This is because RMC models may be conceived as snapshot pictures for representative sections of the structure. In a real system the microscopic structure and the associated conduction pathways are not fixed in time. Their detailed shape and location varies with thermal motion, but pathways of similar characteristics exist at any time somewhere in a macroscopic sample. Thermal vibrations are accounted for by different local distortions in equivalent parts of the model. This replacement of time averaging by space averaging requires a sufficient size of the model to reproduce the characteristic features of local structures. Thus the size of the employed RMC models that consist of 4000 atoms with periodic boundary conditions should be sufficient for the construction of pathway models. Furthermore, since the number of potentially relevant migration barriers in an amorphous system is infinite, the determination of characteristic features of bond-valence pathways has to rely on a statistical description of the total pathway rather than a detailed description of individual migration barriers. Because of the instantaneous distortions contained in RMC models, the modeled Ag^+ correspond to a notable distribution of Ag bond-valences with an average Ag valence of about 10% less than the ideal value $V_{\text{ideal}} = 1$ for a monovalent ion such as Ag^+ . The bond-valence mismatch for equilibrium sites of mobile ions in an ordered crystal structure is typically less than 3%.

RMC models represent fits to experimental data for real samples under well-defined experimental conditions (e.g., temperature) and hence with well-defined properties. For this paper we used RMC produced structural models of crystalline $\alpha\text{-AgI}$ at 525 and 740 K [23], salt doped $(\text{AgI})_{0.75}\text{-}(\text{Ag}_2\text{MoO}_4)_{0.25}$ [24] and $(\text{AgI})_{0.6}\text{-}(\text{Ag}_2\text{O-}2\text{B}_2\text{O}_3)_{0.4}$ [25] glasses, and undoped $\text{Ag}_2\text{O-}2\text{B}_2\text{O}_3$ [25] and $\text{Ag}_2\text{O-}4\text{B}_2\text{O}_3$ [26] glasses. Experimental data and details of the RMC simulations are given elsewhere [23–26]. In brief, the RMC method [21] uses a standard metropolis Monte Carlo algorithm [27], but, instead of minimizing the energy, one minimizes the squared difference between the experimental structure factor and the corresponding structure factor calculated from the computer configuration. In our case, experimental neutron structure factors were obtained over a large Q range (0.2–50 \AA^{-1}) using the wide-angle time-of-flight liquid and amorphous materials diffractometer (LAD) [28] at the pulsed neutron source ISIS, Rutherford-Appleton Laboratory, UK. Corresponding x-ray structure factors were obtained with the high-precision powder diffractometer station 9.1 [29] at SERC's Synchrotron Radiation Source, Daresbury Laboratory,

UK. Hence, the RMC method produces three-dimensional models of disordered materials that agree quantitatively with the available diffraction data (provided that the data do not contain significant systematic errors) and the physical constraints applied, e.g., closest allowed atom-atom distances (see Refs. [23–26] for details about the constraints used).

Conduction pathways for the Ag^+ ions were determined by subdividing the modeled volume into about four million cubic volume elements. Such volume elements are considered as “accessible” for a mobile Ag^+ ion if the bond valence for the hypothetical Ag^+ at its center differs by less than a threshold valence mismatch $|\Delta V|$ from the equilibrium value $V = 1$ or if the sign of the valence deviation changes across the volume element. Since the resolution of about 1000 volume elements per atom is a compromise between the desired accuracy and the computational effort, the second valence mismatch criterion had to be added to cushion the effects of the limited grid resolution (0.2–0.3 \AA , depending on the model). Sites with a distance to other cations M^+ less than the sum of radii $r(\text{Ag}^+) + r(M^+)$ were marked as inaccessible. Accessible volume elements that share common faces or edges belong to the same “pathway cluster.” We found that infinite pathway clusters (i.e., continuous conduction pathways) exist in the RMC “structure snapshots” of all investigated Ag^+ ion conductors for any value of ΔV .

Since only these continuous pathways contribute to the dc conductivity, the volume fraction \mathcal{F} of the continuous pathways was selected to characterize the structural peculiarities of the systems under study. \mathcal{F} is approximated as the fraction of all volume elements that belong to the infinite pathway cluster. We found that systems with different conductivities can be reliably distinguished by this pathway volume fraction \mathcal{F} of the infinite conduction pathways for a fixed valence mismatch threshold $\Delta V = 0.05$, which corresponds to the ΔV required to create a network of bond-valence pathways in the idealized rigid crystal structure of $\alpha\text{-AgI}$. Nevertheless, a different choice of ΔV has no major influence on the ratio between the \mathcal{F} values for different systems. Similarly, we ensured that the comparison of different systems with respect to the pathway volumes was hardly affected by slight changes of the “ideal valence” V .

Thereby a novel strong correlation was established between the ionic conductivity σ of a system at temperature T and its structure expressed by the volume fraction \mathcal{F} of the infinite bond-valence pathway in its RMC model:

$$\log(\sigma T) \propto \sqrt[3]{\mathcal{F}}, \quad (3)$$

as demonstrated in Fig. 1. It can be seen in Fig. 1 that the “pathway volume”–conductivity relation holds for glassy and crystalline systems with silver ion conductivities differing by more than 11 orders of magnitude. The conductivity data were taken from Refs. [1,30–39]. The cube

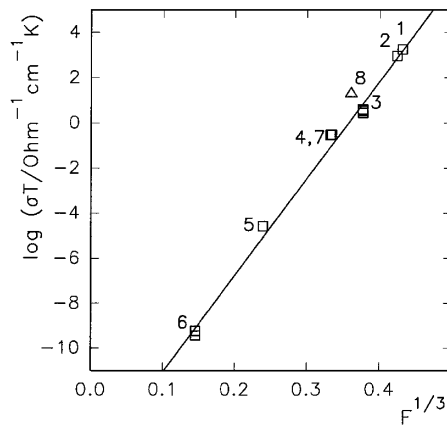


FIG. 1. Correlation between the experimental ionic conductivity σ and the volume fraction \mathcal{F} of the infinite Ag conduction pathway clusters for the RMC models of crystalline AgI at 525 K (1) and at 740 K (2), of the silver-iodide–silver-oxysalt glasses $(\text{AgI})_{0.75}(\text{Ag}_2\text{MoO}_4)_{0.25}$ (3) and $(\text{AgI})_{0.6}(\text{Ag}_2\text{O}-2\text{B}_2\text{O}_3)_{0.4}$ (two models, 4 and 7), as well as of the undoped borate glasses $\text{Ag}_2\text{O}-2\text{B}_2\text{O}_3$ (5) and $\text{Ag}_2\text{O}-4\text{B}_2\text{O}_3$ (6). For comparison, the result for a snapshot from a MD simulation of crystalline $\text{Ag}_{16}\text{I}_{12}\text{P}_2\text{O}_7$ is also included (8). Conductivity data are taken from [30] for (1,2), [31–34] for (3), [1,35] for (4–7), and [38,39] for (8).

root of \mathcal{F} may be thought of as proportional to a mean free path length for the mobile ion. The small influence of temperature on the conductivity of superionic α -AgI, the effects of doping a silver borate network by AgI, and the consequences of different anion networks are all correctly predicted by Eq. (3). The reproducibility of the technique is exemplified in Fig. 1 by two different RMC models of $(\text{AgI})_{0.6}(\text{Ag}_2\text{O}-2\text{B}_2\text{O}_3)_{0.4}$. Other sources for local structural models, such as snapshots from molecular dynamics runs, may be used likewise (cf. the example $\text{Ag}_{16}\text{I}_{12}\text{P}_2\text{O}_7$ [18] in Fig. 1) but might yield less reliable predictions in view of the usually less precise structure.

The experimental activation energy for the ionic conduction E_σ may equally be estimated from the structural model. An increased volume fraction of the infinite pathway reduces the activation energy for an ionic jump according to Fig. 2 which demonstrates that $E_\sigma/k_B T$ varies linearly with the cube root of the bond-valence pathway volume fraction \mathcal{F} . In systems for which several experimental determinations were reported, predictions based on the presented correlation lie within the range of the experimental scatter. Since ionic conduction is basically treated as a geometrical problem in our model, we interpret a reduced activation energy to arise mainly from a reduced strain energy associated with the opening of “doorways” in the structure large enough for the Ag^+ ions to pass through. However, it should be noted that a more detailed analysis would also have to include the partial compensation of the decreasing probability of successful jumps by an increase in the attempt frequency with increasing activation energy [40,41]. As expected

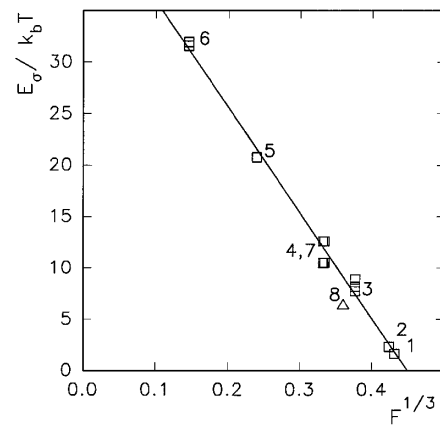


FIG. 2. Correlation between the experimental activation energy for ionic conductivity E_σ and the volume fraction \mathcal{F} of the infinite Ag conduction pathway clusters for the RMC models. Numbers refer to the same samples as in Fig. 1. Experimental data are taken from [30] for (1,2) [31–33] for (3), [35–37] for (4–7), and [38] for (8).

from a synopsis of Figs. 1 and 2, the preexponential factor σ_0 increases slightly with decreasing \mathcal{F} .

Like the elementary network expansion-conductivity relation [16], the presented bond-valence approach emphasizes the importance of “free volume” to the ion mobility. The bond-length bond-valence correlation supplies an empirical measure for weighing this free volume with respect to the shape and connectivity of the voids as well as to the nature of the encompassing counterions. The existence of infinite conduction pathways in all investigated systems is itself an indication for a strongly nonstatistical distribution of the “pathway volume,” as only a few percent of the total volume (1.5% in $\text{Ag}_2\text{O}-4\text{B}_2\text{O}_3$, up to 8% in α -AgI) fulfill the bond-valence sum criterion. Still, the network of conduction pathways is significantly above the percolation threshold for the investigated silver ion conductors.

Only the peripheral regions of large voids belong to the pathway volume. For a given valence mismatch threshold, the thickness of this peripheral layer is determined by the softness of the Ag-X bond-valence pseudopotential, i.e., by the polarizabilities of the X anions. For ions with high polarizabilities the same bond-valence interval corresponds to a larger bond-distance interval, which explains why highly polarizable ions promote the ionic conduction. In Eq. (2) the differences in the anion polarizabilities are accounted for explicitly by the different denominators of the bond-valence parameter sets. This permits a discrimination of the contributions of differently coordinated Ag^+ ions to the long-range ion conductivity in silver-iodide–silver-oxide-based glasses [19].

As demonstrated qualitatively for the glass system $(\text{AgI})_{0.75}(\text{Ag}_2\text{MoO}_4)_{0.25}$ in Fig. 3, the distribution of accessible sites with predominant coordination by iodide or oxide is clearly nonstatistical. In accordance with our previous findings for crystalline Ag^+ conductors in the

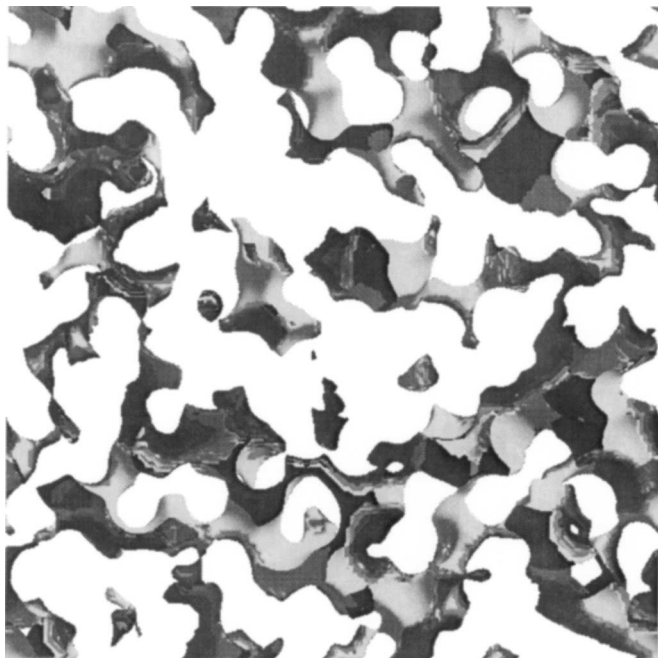


FIG. 3. A 2 Å thick slice through the bond-valence pathway model of $(\text{AgI})_{0.75}(\text{Ag}_2\text{MoO}_4)_{0.25}$ for $|\Delta V| = 0.05$. Light parts of the pathway surface correspond to mainly iodide coordinated Ag^+ sites, while dark regions represent mainly oxide coordinated sites.

systems $\text{AgI-Ag}_4\text{V}_2\text{O}_7$ [42] and $\text{AgI-Ag}_4\text{P}_2\text{O}_7$ [43], regions of mainly iodide coordinated sites bridged by mainly oxide coordinated sites are a common characteristic of the modeled network of pathways. Pathways consisting only of iodide coordinated sites, as postulated earlier by Minami and co-workers [7,44], can be ruled out in this system. A quantitative investigation on this aspect for various glass systems is in preparation [45].

We are grateful to Dr. R. L. McGreevy for the RMC configurations of $\alpha\text{-AgI}$ at 525 and 740 K and to Professor L. Börjesson for experimental neutron diffraction data on silver borate glasses. Financial support to J. S. from the Swedish Natural Science Research Council and to St. A. from the Deutsche Forschungsgemeinschaft is gratefully acknowledged.

-
- [1] A. Schiraldi and E. Pezzati, *Mater. Chem. Phys.* **23**, 75 (1989).
 [2] T. Saito *et al.*, *Solid State Ion.* **86–88**, 491 (1996).
 [3] D. Ravaine and J. L. Souquet, *Phys. Chem. Glasses* **18**(2), 27 (1977).
 [4] A. M. Glass and K. Nassau, *J. Appl. Phys.* **51**, 3756 (1980).

- [5] P. Maass, A. Bunde, and M. D. Ingram, *Phys. Rev. Lett.* **68**, 3064 (1992).
 [6] G. Carini *et al.*, *Phys. Rev. B* **29**, 3567 (1984).
 [7] T. Minami, *J. Non-Cryst. Solids* **73**, 273 (1985).
 [8] G. N. Greaves, *J. Non-Cryst. Solids* **71**, 203 (1985).
 [9] M. Tachez *et al.*, *Solid State Ion.* **18–19**, 372 (1986).
 [10] A. Fontana, F. Rocca, and M. P. Fontana, *Phys. Rev. Lett.* **58**, 503 (1987).
 [11] C. Rousselot *et al.*, *Solid State Ion.* **78**, 211 (1995).
 [12] M. D. Ingram, *Philos. Mag. B* **60**, 729 (1989); *Mater. Chem. Phys.* **23**, 51 (1989).
 [13] J. Kincs and S. W. Martin, *Phys. Rev. Lett.* **76**, 70 (1996).
 [14] J. O. Isard, *J. Non-Cryst. Solids* **1**, 235 (1969).
 [15] M. D. Ingram, *Phys. Chem. Glasses* **28**, 215 (1987).
 [16] J. Swenson and L. Börjesson, *Phys. Rev. Lett.* **77**, 3569 (1996).
 [17] J. D. Garrett *et al.*, *J. Solid State Chem.* **42**, 183 (1982).
 [18] St. Adams and J. Maier, *Solid State Ion.* **105**, 67 (1998).
 [19] St. Adams, *Solid State Ion.* (to be published).
 [20] I. D. Brown, *Acta Crystallogr. Sect. B* **48**, 553 (1992).
 [21] R. L. McGreevy and L. Pusztai, *Mol. Simul.* **1**, 359 (1988).
 [22] S. F. Radaev, L. Fink, and M. Trömel, *Z. Kristallogr. Suppl.* **8**, 628 (1994); M. Trömel, (private communication).
 [23] V. M. Neild *et al.*, *Solid State Ion.* **66**, 247 (1993).
 [24] J. Swenson *et al.*, *J. Phys. Condens. Matter* **8**, 3545 (1996).
 [25] J. Swenson *et al.*, *Phys. Rev. B* **55**, 11 236 (1997).
 [26] J. Swenson, L. Börjesson, and W. S. Howells, *J. Phys. Condens. Matter* **11**, 9275 (1999).
 [27] N. Metropolis *et al.*, *J. Phys. Chem.* **21**, 1087 (1953).
 [28] W. S. Howells, Rutherford-Appleton Laboratory Report No. RAL-86-042, 1986.
 [29] G. Buchnell-Wye and R. J. Cernik, *Rev. Sci. Instrum.* **63**, 1001 (1992).
 [30] A. Kvist and A.-M. Josefson, *Z. Naturforsch.* **23A**, 625 (1968).
 [31] J. Kawamura and M. Shimoji, *J. Non-Cryst. Solids* **88**, 281 (1986).
 [32] M. C. R. Shastri and K. J. Rao, *Solid State Ion.* **37**, 17 (1989).
 [33] St. Adams, K. Hariharan, and J. Maier, *Solid State Ion.* **86–88**, 503 (1996).
 [34] C. A. Angell, *Solid State Ion.* **18–19**, 72 (1986).
 [35] G. Chiodelli *et al.*, *Solid State Ion.* **8**, 311 (1983).
 [36] G. Chiodelli *et al.*, *J. Non-Cryst. Solids* **51**, 143 (1982).
 [37] G. Carini *et al.*, *Phys. Rev. B* **30**, 7219 (1984).
 [38] M. Sayer *et al.*, *J. Solid State Chem.* **42**, 191 (1982).
 [39] M. N. Avashti, M. Saleem, and M. T. El-Gemal, *Solid State Ion.* **6**, 43 (1982).
 [40] W. Meyer and H. Neldel, *Z. Tech.* **18**, 588 (1937).
 [41] K. Ngai, *Solid State Ion.* **105**, 231 (1998).
 [42] St. Adams, *Z. Kristallogr.* **211**, 770 (1996).
 [43] St. Adams and A. Preusser, *Acta Crystallogr. Sect. C* **55**, 1741 (1999).
 [44] T. Minami and M. Tanaka, *J. Non-Cryst. Solids* **38–39**, 289 (1980).
 [45] St. Adams and J. Swenson (to be published).